

# Antiferrodistortive Order in the New Solid Solution $\text{CrZr}_{0.75}\text{Nb}_{0.25}\text{F}_6$

F. Goubard,<sup>1</sup> S. Llorente, D. Bizot, J. Chassaing, and M. Quarton

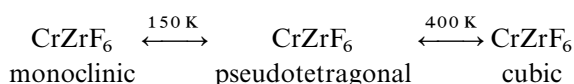
Laboratoire de Cristalochimie du Solide, CNRS-URA 1388, Université Pierre et Marie Curie, 4 place Jussieu, 75252 Paris Cedex 05, France

Received November 21, 1996; in revised form February 20, 1997; accepted February 20, 1997

The new compound  $\text{CrZr}_{0.75}\text{Nb}_{0.25}\text{F}_6$  has been synthesized. Structural determination by the Rietveld full-profile technique has been carried out on powdered samples. This compound crystallizes in the orthorhombic system, space group *Pnma*, with  $a=11.5728(4)$  Å,  $b=7.9671(2)$  Å, and  $c=5.8203(2)$  Å. The structure displays an antiferrodistortive order of elongated  $\text{CrF}_6$  octahedra induced by a cooperative Jahn–Teller effect. This result is compared with ferrodistoritive order of  $\text{CrF}_6$  octahedra in the HT  $\text{CrNbF}_6$  form. The magnetic behavior of both  $\text{CrNbF}_6$  and  $\text{CrZr}_{0.75}\text{Nb}_{0.25}\text{F}_6$  at low temperature is described. © 1997 Academic Press

## INTRODUCTION

This work concerns the fluorocomplexes of niobium(IV) (1–4) and is a part of a more general study of the second row transition element fluorides. In this paper, emphasis will be put on the influence of the Jahn–Teller  $\text{Cr}^{2+}$  cation on the structure of  $\text{CrMF}_6$  compounds ( $M = \text{Zr}, \text{Nb}$ ).  $\text{CrNbF}_6$  (1) has been shown to derive from the  $\text{ReO}_3$  type by a strong cooperative Jahn–Teller distortion leading to a ferrodistoritive order of tetragonally elongated  $\text{CrF}_6$  octahedra ( $c/a > 1$ ).  $\text{CrZrF}_6$  is trimorphous: the high temperature (HT) variety is cubic, whereas distortions occur at low temperature, giving rise to two additional Jahn–Teller structural modified types which are pseudotetragonal and monoclinic (5):

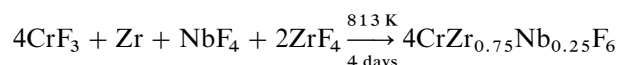


The purpose of this study is to characterize the crystal structure of the room temperature (RT) form and to compare it to the  $\text{CrNbF}_6$  structure.

## EXPERIMENTAL METHODS

The fluoride  $\text{CrZrF}_6$  was obtained as a green powder by reacting the stoichiometric mixture  $3\text{ZrF}_4 + \text{Zr}(\text{foil}) +$

$4\text{CrF}_3$  at 1073 K for 4 days. The solid solution  $\text{CrZr}_{0.75}\text{Nb}_{0.25}\text{F}_6$  was prepared by the following solid-state reaction:



All samples were heated in copper tubes sealed under dry argon. Because of the very high hygroscopicity of  $\text{NbF}_4$  and fluoroniobates, all handling was performed in a dry glove box filled with nitrogen. The reaction products (slightly green-colored powders) were characterized at 293 K by their X-ray powder diffraction patterns with  $\text{CoK}\alpha$  radiation ( $\lambda = 1.7909$  Å) using silicon as internal standard ( $a = 5.4308$  Å). Structural studies were carried out on powder samples, peak profiles were calculated with the Voigt function, and diffraction patterns were analyzed by type profile refinement using the Rietveld method (6) with the Fullprof program (7).

The phase transitions were characterized by DTA measurements (temperature cycling  $10\text{ K min}^{-1}$ ) and temperature-dependent X-ray diffraction (Bragg–Brentano configuration, evacuated chamber with a Kapton window, Ni-filtered  $\text{CuK}\alpha$  radiation,  $\lambda = 1.54178$  Å).

Magnetic susceptibility was measured in the temperature range 4.2–300 K with a MANICS DSM8 magnetometer. The applied field was  $0 \leq H \leq 17$  kOe. Diamagnetic corrections for  $\text{CrNbF}_6$  and  $\text{CrZr}_{0.75}\text{Nb}_{0.25}\text{F}_6$  are respectively  $-91 \times 10^{-6}$  and  $-75 \times 10^{-6} \text{ cm}^3 \text{ mol}^{-1}$ .

## STRUCTURAL STUDIES

### $\text{CrZrF}_6$

By analogy with  $\text{CuZrF}_6$ , Reinen (8) has suggested the existence of an antiferrodistortive order of elongated  $\text{CrF}_6$  octahedra in the pseudotetragonal form of  $\text{CrZrF}_6$ . It is difficult to determine the symmetry of this room temperature form with certainty from the X-ray diffraction analysis because the cubic and pseudotetragonal phases coexist in the sample at 293 K (Fig. 1).

In order to specify the transition characteristics, a temperature-dependent study has been carried out. DTA

<sup>1</sup>To whom correspondence should be addressed.

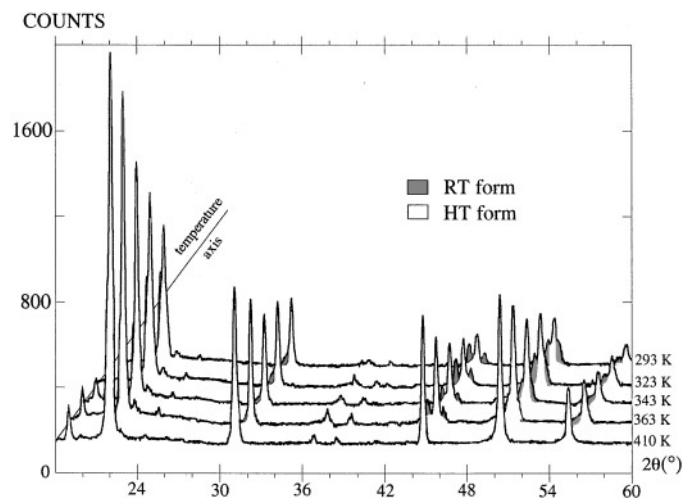


FIG. 1.  $\text{CrZrF}_6$  powder diffraction pattern vs temperature.

experiments show a slight and progressive change with temperature without a notable thermic effect. By X-ray powder diffraction the cubic form of  $\text{CrZrF}_6$  (space group  $Fm\bar{3}m$ ) appears pure above 400 K (Fig. 1). A quantitative analysis of the X-ray diffraction peaks (400) of the cubic form and (331) of the RT form was undertaken. From these results (Fig. 2), we noticed that the transformation proceeds only while the temperature changes and stops if the compound is kept at constant temperature. So the transition is athermal: the ratio of transformed  $\text{CrZrF}_6$  is a function of temperature alone. We can compare this transformation to the martensitic one in which a cooperative and progressive displacement of atoms of the parent phase (HT form) leads to the growth of a new phase. At 100 K both RT and HT forms are always present, without evidence of a low temperature form.

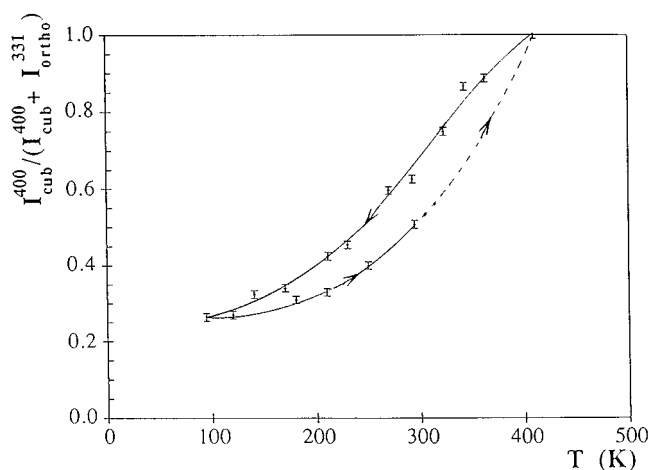


FIG. 2. Thermal evolution of (400) peak intensity of  $\text{CrZrF}_6$  cubic form.

A careful analysis of diffractograms has allowed the unambiguous attribution of diffraction peaks to each phase. At 293 K their crystallographic characteristics were extracted by performing full-profile fits on the corresponding diffraction pattern:

– HT form: cubic, space group  $Fm\bar{3}m(9)$ ,  $a_c = 8.124(1) \text{ \AA}$ ,  $V = 536.1(1) \text{ \AA}^3$ ,  $Z = 4$ .

– RT form: orthorhombic, space group  $Pnma$ ,  $a_0 = 11.571(2) \text{ \AA}$ ,  $b_0 = 8.0166(8) \text{ \AA}$ ,  $c_0 = 5.7671(7) \text{ \AA}$ ,  $V = 535.0(1) \text{ \AA}^3$ ,  $Z = 4$ .

It should be observed that the relations  $a_c \approx a_0/\sqrt{2} \approx b_0 \approx c_0\sqrt{2}$  are in agreement with the displacive nature of the transformation between RT and HT forms. Likewise the relation  $a_0 \approx 2c_0$  agrees with the designation “pseudotetragonal” proposed by Reinen (8) for the RT phase.

At room temperature, no precise structural research was possible because reflections were too close to each other, and it was necessary to stabilize the RT form by a partial cationic substitution. With a similar ionic radius, the niobium(IV) ion ( $r = 0.68 \text{ \AA}$ ) is a good choice as a substitute for the zirconium(IV) ion ( $r = 0.72 \text{ \AA}$ ). So, by X-ray diffraction, a exploration of the binary system  $\text{CrNbF}_6\text{--CrZrF}_6$  was undertaken at 293 K (Fig. 3). Substitution in the  $\text{CrNbF}_6$  host lattice yields a tetragonal disordered solid solution  $\text{CrNb}_{1-x}\text{Zr}_x\text{F}_6$  ( $\approx 0.05 \leq x \leq 0.34$ ) which is isotypic with the HT form of  $\text{CrNbF}_6$ . Below  $x \approx 0.05$  the solid solution is monoclinic. In the composition range  $0.34 < x < 0.75$ , we obtained a mixture of tetragonal  $\text{CrNb}_{0.66}\text{Zr}_{0.34}\text{F}_6$  and orthorhombic  $\text{CrZr}_{0.75}\text{Nb}_{0.25}\text{F}_6$ . At higher concentrations ( $0.75 \leq x \leq 1$ ), a monophasic domain corresponding to the orthorhombic solid solution isotypic to the RT variety of  $\text{CrZrF}_6$  is observed.

Structural research has been devoted to the limit of solid solution:  $\text{CrZr}_{0.75}\text{Nb}_{0.25}\text{F}_6$ .

### $\text{CrZr}_{0.75}\text{Nb}_{0.25}\text{F}_6$

X-ray powder diffraction data were collected at 293 K, using an airtight sample holder equipped with a beryllium window. Results of structural refinements are summarized in Tables 1 and 2. The observed, calculated, and difference X-ray diffraction profiles are presented in Fig. 4.

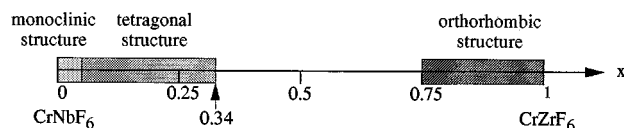


FIG. 3. Existence fields for solid solutions  $\text{CrNb}_{1-x}\text{Zr}_x\text{F}_6$  ( $0 \leq x \leq 1$ ) vs composition at 293 K.

**TABLE 1**  
Atomic Parameters for CrZr<sub>0.75</sub>Nb<sub>0.25</sub>F<sub>6</sub>

$a = 11.5728(4) \text{ \AA} \quad b = 7.9671(2) \text{ \AA} \quad c = 5.8202(2) \text{ \AA}$ $V = 536.6(1) \text{ \AA}^3 \quad Z = 4$					
Atom	Wyckoff position	Coordinate			Thermal agitation factor $B (\text{ \AA}^2)$
		$x$	$y$	$z$	
Zr/Nb	4c	0.373(1)	1/4	0.772(2)	0.6(1)
Cr	4c	0.126(1)	1/4	0.249(1)	0.3(2)
F(1)	4c	0.998(2)	1/4	0.980(2)	1.2(2)
F(2)	4c	0.997(2)	1/4	0.482(2)	2.1(2)
F(3)	4c	0.751(2)	1/4	0.481(2)	0.3(2)
F(4)	4c	0.752(2)	1/4	0.982(2)	1.2(2)
F(5)	8d	0.125(1)	0.504(2)	0.263(1)	2.1(2)

Note.  $R_B = 6.43\%$ ;  $R_P = 17.1\%$ ;  $R_F = 9.51\%$ ;  $R_{WP} = 14.0\%$ .

The 3D framework (Fig. 5) is built up from corner-sharing Zr(Nb)F<sub>6</sub> and CrF<sub>6</sub> distorted octahedra forming pseudo-linear chains ( $\text{Nb}^{4+}/\text{Zr}^{4+}-\text{F}-\text{Cr}^{2+} = 179.5^\circ$ ) running along the three axes of the cell. The structural analysis of CrZr<sub>0.75</sub>Nb<sub>0.25</sub>F<sub>6</sub> reveals quasi-tetragonally elongated CrF<sub>6</sub> octahedra characterized by a distinct orthorhombic component with three different types of Cr–F bond lengths (Table 3):  $d_x = 2.14\text{--}2.16 \text{ \AA}$ ,  $d_y = 2.025 \text{ \AA}$ , and  $d_z = 1.97\text{--}2.02 \text{ \AA}$ . While the  $d_y$  bond order is parallel to the

**TABLE 2**  
X-Ray Powder Diffraction Data for CrZr<sub>0.75</sub>Nb<sub>0.25</sub>F<sub>6</sub>

$hkl$	$d_{\text{obs}} (\text{ \AA})$	$(I/I_0)_{\text{obs}}$	$(I/I_0)_{\text{cal}}$
101	5.199	2	1
011	4.700	9	8
210	4.682	7	8
111	4.353	1	1
201	4.104	100	100
020	3.984	71	70
002	2.9102	5	5
400	2.8933	5	5
221	2.8583	44	43
212	2.4719	2	2
411	2.4641	3	3
031/230	2.4147	2	2
022	2.3502	2	2
420	2.3406	2	2
312	2.2303	0	1
402	2.0520	27	27
223	1.6700	7	7
621	1.6635	8	8
042	1.6437	2	2
440	1.6406	2	2
612	1.5758	1	1

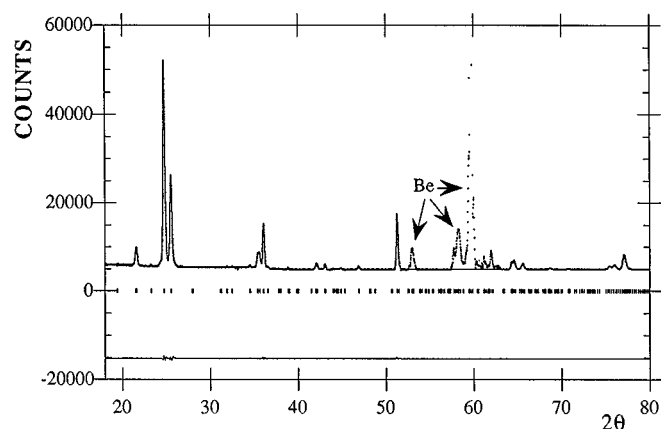


**FIG. 4.** Observed (crosses) and calculated (full curve) powder diffraction profile of CrZr<sub>0.75</sub>Nb<sub>0.25</sub>F<sub>6</sub> at room temperature. The short vertical lines below the profiles mark the positions of all possible Bragg reflections. The lower curve shows the difference between observed and calculated profiles.

pseudotetragonal  $b$ -axis, and  $d_x$  ( $d_z$ ) bonds of neighboring CrF<sub>6</sub> polyhedra in the (010) planes are oriented perpendicular to each other (Fig. 6). This kind of cooperative order is called antiferrodistortive.

A unit cell with an antiferrodistortive order of tetragonally elongated octahedra can be described as consisting of two ferrodistoritive sublattices which are rotated by  $\pi/2$  from each other (9). This kind of symmetry has been also observed for KCrF<sub>3</sub> and for Jahn–Teller Cu<sup>2+</sup> compounds such as KCuF<sub>3</sub> (10), K<sub>2</sub>CuF<sub>4</sub> (11), and Ba<sub>2</sub>CuF<sub>6</sub> (12).

By comparison, in CrNbF<sub>6</sub> and CrF<sub>6</sub> octahedra are also tetragonally elongated, but all their long axes are oriented parallel to the  $c$ -axis in the tetragonal modification. This symmetry in the cooperative Jahn–Teller effect is called ferrodistoritive. Otherwise, the large Cr–F bonds are shorter

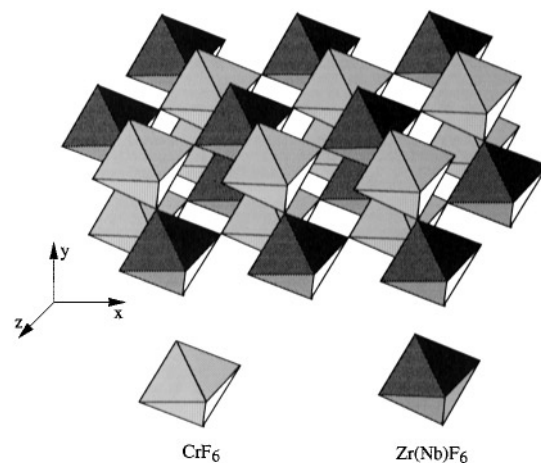


**FIG. 5.** Perspective view of the CrZr<sub>0.75</sub>Nb<sub>0.25</sub>F<sub>6</sub> structure.

**TABLE 3**  
Interatomic Distances (Å) in Some Fluoride Compounds

	CrZr <sub>0.75</sub> Nb <sub>0.25</sub> F <sub>6</sub> (This work)	MZrF <sub>6</sub> (13)	CrNbF <sub>6</sub> (1)	KCrF <sub>3</sub> (16)	Sum of ionic radii (15)
Cr–F (Å)	2.16(1)				
	2.14(1)	—	2.39(3)	2.32	
	1.97(1)		× 2	1.95	2.085
	2.02(1)		2.01(2)	2.00	
	2.025(5) × 2		× 4		
Zr, Nb–F (Å)	2.02(1)				
	2.03(1)	1.98 to	1.92(2)		2.005(Zr)
	2.04(1)	2.03	× 4		1.965(Nb)
	2.06(1)		1.82(3)		
	1.961(5) × 2		× 2		

than CrNbF<sub>6</sub> bonds. This result agrees with several considerations: the Zr(IV) ion is larger than the Nb(IV) ion and so Cr–F bonds must be stronger in CrZrF<sub>6</sub> than in CrNbF<sub>6</sub>; the HT cubic phase of CrZrF<sub>6</sub> exists and is stable below 400 K, whereas CrF<sub>6</sub> octahedra in CrNbF<sub>6</sub> are so distorted that it is impossible to obtain a more symmetric variety at high temperature before decomposition at 873 K.

The Zr(Nb)F<sub>6</sub> octahedra are tetragonally flattened with two axial short bond lengths and four longer ones; their interatomic distances are in excellent agreement with those of other MZrF<sub>6</sub> type compounds (Table 3).

### MAGNETIC STUDIES

Whereas VNbF<sub>6</sub> and MnNbF<sub>6</sub> (LiSbF<sub>6</sub>-type) exhibit ferrimagnetic behavior, our investigation of the magnetic properties of CrNbF<sub>6</sub> shows that the anisotropic Cr<sup>2+</sup> ion induces antiferromagnetic behavior ( $T_N \approx 52$  K) (Fig. 7).

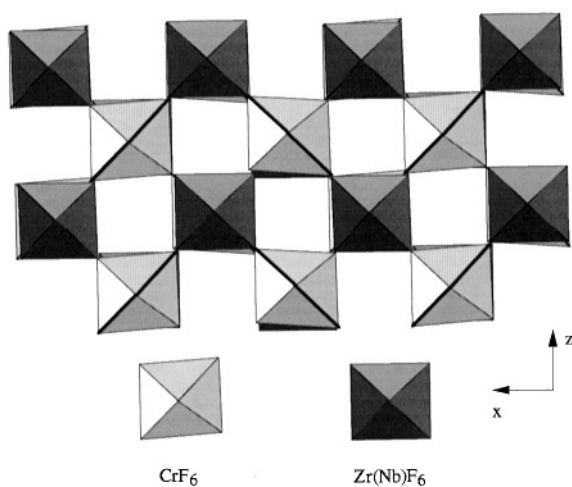


**FIG. 6.** Projection along [010] of the polyhedral crystal structure of CrZr<sub>0.75</sub>Nb<sub>0.25</sub>F<sub>6</sub>. The broad lines materialize the large Cr–F bond lengths.

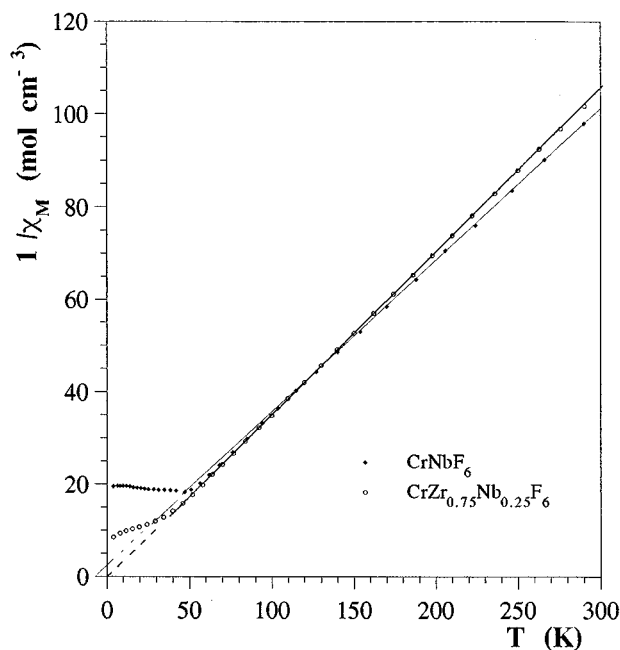


**FIG. 7.** Thermal variation of  $\chi_M^{-1}$  for CrNbF<sub>6</sub> (·) and for CrZr<sub>0.75</sub>Nb<sub>0.25</sub>F<sub>6</sub> (◦).

The Curie–Weiss law is well obeyed above 52 K, which yields a molar Curie constant  $C_M(\text{exp}) = 2.99 \text{ cm}^3 \text{ K mol}^{-1}$  and  $\theta_p = -6$  K. We have also studied the magnetic properties of CrZr<sub>0.75</sub>Nb<sub>0.25</sub>F<sub>6</sub> (Fig. 7): no minimum appears on the  $\chi_M^{-1}$  vs  $T$  curve, but only a deviation from the Curie–Weiss law below 40 K. In the paramagnetic range, the values  $C_M = 2.84 \text{ cm}^3 \text{ K mol}^{-1}$  and  $\theta_p \approx 0$  K are in agreement with the weakening of magnetic interactions as a consequence of the paramagnetic species dilution.

The experimental values of  $C_M$  in the paramagnetic range are somewhat smaller than the theoretical values ( $C_{\text{Meal}} = 3 (\text{Cr}^{2+}) + (1-x) 0.375 (\text{Nb}^{4+}) = 3.375 \text{ cm}^3 \text{ K mol}^{-1}$  for CrNbF<sub>6</sub> and  $3.094 \text{ cm}^3 \text{ K mol}^{-1}$  for CrZr<sub>0.75</sub>Nb<sub>0.25</sub>F<sub>6</sub>), like those for the ferrimagnetic VNbF<sub>6</sub> and MnNbF<sub>6</sub> compounds (2, 14). The antiferromagnetic behavior of CrNbF<sub>6</sub> might arise from superexchange interactions,  $b_{2g}(\text{Nb}^{4+}) - p\pi(F^-) - b_{2g}(\text{Cr}^{2+})$ , because these octahedra exhibit a  $D_{4h}$  symmetry; however, one cannot rule out the hypothesis of long-range Cr<sup>2+</sup>–Cr<sup>2+</sup> magnetic interactions.

### CONCLUSION

Unlike the ferrodistorive order in CrNbF<sub>6</sub>, the Cr<sup>2+</sup> cation induces in CrZr<sub>0.75</sub>Nb<sub>0.25</sub>F<sub>6</sub> (isotypic with the room temperature form of CrZrF<sub>6</sub>) an antiferrodistorive Jahn–Teller ordering. The energy difference between the two cooperative patterns seems very small: a tiny perturbation induced by a partial cationic substitution is sufficient to alter the ordering symmetry.

## REFERENCES

1. F. Goubard, D. Bizot, J. Chassaing, and M. Quarton, *Eur. J. Solid State Inorg. Chem.* **31**, 223 (1994).
2. F. Goubard, T. Le Mercier, J. Chassaing, D. Bizot, M. Quarton, and G. André, *J. Magn. Magn. Mater.* **146**, 129 (1995).
3. J. Chassaing, D. Bizot, and C. Monteil, *J. Solid State Chem.* **43**, 327 (1982).
4. D. Bizot, J. Chassaing, J. Pannetier, M. Leblanc, A. Le Bail, and G. Ferey, *Solid State Commun.* **58**(1), 71 (1986).
5. D. Reinen and F. Steffens, *Z. Anorg. Allg. Chem.* **441**, 63 (1978).
6. H. M. Rietveld, *J. Appl. Crystallogr.* **2**, 65 (1969).
7. J. Rodriguez-Carvajal, 'FULLPROF: A program for Rietveld refinement and pattern matching analysis', in "Abstracts of the Satellite Meeting on Power Diffraction of the XV Congress of the IUCr," p. 127, Toulouse, France, 1990.
8. C. Friebel, J. Pebler, F. Steffens, M. Weber, and D. Reinen, *J. Solid State Chem.* **46**, 253 (1983).
9. H. W. Mayer, D. Reinen, and G. Heger, *J. Solid State Chem.* **50**, 213 (1983).
10. D. Reinen and C. Friebel, *Struct. Bonding* **37**, 1 (1979).
11. R. Haegele and D. Babel, *Z. Anorg. Allg. Chem.* **409**, 11 (1974).
12. H. G. von Schnering, *Z. Anorg. Allg. Chem.* **400**, 201 (1973).
13. M. Poulain, *Thèse de doctorat d'Etat*, Université de Rennes, 1973.
14. V. Delobbe, J. Chassaing, D. Bizot, M. Quarton, P. Lacorre, Y. Calage, M. Leblanc, and G. Ferey, *J. Magn. Magn. Mater.* **74**, 165 (1988).
15. R. D. Shannon, *Acta Crystallogr. Sect. A* **32**, 752 (1976).
16. D. Oelkrug, *Struct. Bonding* **9**, 1 (1971).